Available online at www.sciencedirect.com
ScienceDirect
Journal of Sound and Vibration 303 (2007) 675–690
JOURNAL OF SOUND AND VIBRATION
www.elsevier.com/locate/jsvi

A hybrid method for vibroacoustics based on the radiative energy transfer method

E. Sadoulet-Reboul[a,*], A. Le Bot[b], J. Perret-Liaudet[b], M. Mori[c], H. Houjoh[c]

[a]*Laboratoire de Tribologie et Dynamique des Systèmes, Ecole Nationale d'Ingénieurs de Saint Etienne, 58 rue Jean Parot, 42023 Saint Etienne Cedex 2, France*

[b]*Laboratoire de Tribologie et Dynamique des Systèmes, Ecole Centrale de Lyon, 36 avenue Guy de Collongue, 69134 Ecully Cedex, France*

[c]*Precision and Intelligence Laboratory, Tokyo Institute of Technology, 4259 Nagatsuta-cho, Midori-ku, Yokohama 226-8503, Japan*

Received 27 February 2006; received in revised form 14 December 2006; accepted 23 January 2007
Available online 23 March 2007

Abstract

A hybrid method is proposed to predict the noise radiated in the high-frequency range by a structure whose vibratory behavior is rather in the low-frequency range. This problem meets for instance when the structure radiates inside some closed acoustical spaces. The proposed approach is called hybrid as it couples two methods valid on different frequency bands respectively used for the structural and acoustical systems. Low-frequency structural approaches generally provide the velocity field on the vibrating surface while methods adapted to high-frequency acoustical studies are based on energy data: so the main difficulty for the coupling is a problem of data compatibility. In the proposed hybrid method, the radiated noise is predicted by using the radiative energy transfer method which is an energy boundary integral method basically equivalent to the known ray-tracing method for acoustic applications. Adequate equivalent energy sources are estimated on the surface of the vibrating structure from the surface pressure and velocity fields. These sources are then introduced in the integral equation of the radiative energy transfer method. The approach is applied to predict the radiation of a ribbed plate sandwiched between two absorbant panels: good agreement is observed with the results given by the boundary element method. Generally speaking, the hybrid method can be considered to apply the radiative energy transfer method for high-frequency acoustical predictions from the knowledge of the vibratory behavior of a structure.

1. Introduction

The prediction of sound radiation from the surface of a vibrating structure has given rise to the development of various vibroacoustic methods depending on the context and depending on the frequency. The finite element method (FEM) [1] can be used to solve both the structural and acoustical problems but it requires that

Abbreviations: BEM, boundary element method; EBEM, energy boundary element method; EFEA, energy finite element analysis; EFEM, energy finite element method; ESSM, energy source simulation method; FACI, frequency averaged cross intensity; FACP, frequency averaged cross pressure; FACV, frequency averaged cross velocity; FEM, finite element method; SEA, statistical energy analysis.

*Corresponding author. Tel.: +33 4 77 43 75 88; fax: +33 4 77 43 75 39.
E-mail address: Emeline.Sadoulet@enise.fr (E. Sadoulet-Reboul).

0022-460X/$ - see front matter © 2007 Elsevier Ltd. All rights reserved.
doi:10.1016/j.jsv.2007.01.031

Nomenclature

c	speed of sound
$d = \|\mathbf{q}' - \mathbf{q}\|$	distance between the source points $\mathbf{q}$ and $\mathbf{q}'$
g	Green's function
G	kernel function for energy density
H	kernel function for energy intensity
$\mathbf{I}$	acoustical intensity
I_n	normal intensity
j	imaginary number such that $j^2 = -1$
k	complex wavenumber
k_0	real part of the complex wavenumber
m	atmospheric attenuation factor
$\mathbf{n_p}$, $\mathbf{n_{p'}}$, $\mathbf{n_q}$, $\mathbf{n_{q'}}$	unit outward normal at point $\mathbf{p}$, $\mathbf{p}'$, $\mathbf{q}$, $\mathbf{q}'$
p	sound pressure
$\mathbf{p}$, $\mathbf{p}'$, $\mathbf{q}$, $\mathbf{q}'$, $\mathbf{s}$	source position
r, r'	source–receiver distance
$\mathbf{r}$	receiver position
R_{pp}	pressure cross-spectral density
$R_{\gamma\gamma}$	acceleration cross-spectral density
$R_{\gamma p}$	intensity cross-spectral density
Re	real part of a complex number
S	vibrating surface
$\mathbf{u}$, $\mathbf{u}'$	unit vector from a source point to the receiver point
W	acoustical energy density
α	absorption coefficient
γ_n	normal acceleration
Γ	boundary surface of Ω
ρ_0	air density
σ	surface source located on Γ
σ_f	fictitious source located on Γ
σ_e	equivalent source located on S
σ_{pp}	pressure source located on S
$\sigma_{\gamma\gamma}$	velocity source located on S
$\sigma_{\gamma p}$	intensity source located on S
θ, θ'	angle between the direction of emission $\mathbf{u}$, $\mathbf{u}'$ and the outward normal $\mathbf{n_p}$, $\mathbf{n_{p'}}$ at point $\mathbf{p}$, $\mathbf{p}'$
Θ	emission angle from the source point $\mathbf{q}$
ω	angular frequency
Ω	acoustical domain
$*$	conjugate of a complex number

all the three-dimensional fluid domain surrounding the structure be discretized. The boundary element method (BEM) [2] is generally preferred especially for free-field radiation problems as the radiated field depends in this case on the surface fields, and thus only the problem's boundaries need to be discretized. For many applications, the vibratory field originates from a FEM analysis and the BEM is then used to compute the radiated field. Nevertheless, even with the BEM, the number of mesh points increases dramastically as the frequency increases and both methods lead to large computional times.

To overcome this problem, several energy methods have emerged to extend the vibroacoustic predictions to higher frequency bands. Viktorovitch [3,4] obtains integral formulations over the product of the classical displacement variable from the classical integral equations. In another way, a BEM based on energy quantities is developed by Guyader [5–8], Kim and Ih [9–11], and Wang et al. [12,13]. Guyader derives an integral equation for frequency averaged quadratic pressure on the assumption of statistical independence of Green's function and boundary pressure and velocity of the radiating object. Three kinds of sources are introduced including cross contributions, the cross velocity source (FACV), the cross intensity source (FACI), and the cross pressure source (FACP). Similar formulations and sources are used in the simplified BEM developed by Kim and Ih: one main difference is that the correlation coefficient between two different surface points is assumed to be small enough so that cross contributions between two different points be neglected. Besides, the non-uniqueness problem which still appears in the integral equation developed by Guyader is removed in the simplified BEM. It is found that the mesh size is larger than with the BEM, and the assembling time of the method is quite small compared with the BEM. One similarity between these energy methods and the BEM is that specific boundary integral equations must be solved firstly to get the acoustical field at any point of the acoustic domain. The solving of these equations is particularly time-consuming as it involves the inversion of a complex fully populated matrix. For interior problems or when the vibrating structure is located inside a complex acoustical domain with many boundaries, the CPU-time for this inversion is all the higher as all the boundaries must be discretized leading to huge matrix to invert. In general, field point processing is quite fast for a reasonable number of points.

Some other methods based on energy quantities have emerged to study the noise radiated by a vibrating structure in an unbounded medium. The energy boundary element method (EBEM) developed by Wang et al. [12,13] converts the phase dependent variables of the BEM into the acoustic intensity boundary conditions by applying an ensemble averaging operator on the BEM integral equations. The intensity boundary conditions originates from an energy finite element analysis (EFEA) to compute the structural vibration of the structure. As in the simplified BEM, surface sources are incoherent and the cross terms are zero. Recently, the equivalent source method [14–16] has also been extended by Herrin et al. [17] on the basis of energy considerations. In the energy source simulation method (ESSM), a set of energy sources is introduced and their strengths are found by minimizing the difference between a specified intensity boundary condition on the surface of the vibrating structure and the energy field generated by the sources. One limitation with the ESSM as with the simplified BEM is that the directivity characteristics of the energy field are not reproduced due to the uncorrelation assumption.

This paper focuses on the prediction of the noise radiated in the high-frequency range by a structure vibrating in the low-frequency range. For a structure vibrating inside a closed enclosure with pure-tone excitation, only few vibratory modes for the structure are likely to be excited such that its vibratory behavior lies in the low-frequency range and can be determined using standard methods generally based on modal approaches. However, depending in particular on the size of the cavity, the number of acoustical modes excited inside the enclosure is likely to be high such that the acoustical behavior of this same structure lies no longer in the high-frequency range. Thus, the method proposed in this paper to solve such a problem is called hybrid as it couples two methods valid on different frequency bands. The development of hybrid approaches is quite recent: amongst, the work of Langley and Bremner [18] for the study of complex dynamic systems is a hybrid method between a determinist approach and the statistical energy analysis (SEA), and the works of Lee et al. [19] and of Jayachandra and Bonhila [20] for vibroacoustic applications are, respectively, based on the coupling between the energy finite element method (EFEM) or the SEA for vibratory study and the BEM or acoustic modal summation for acoustics. In the hybrid approach proposed in this paper for a structural/acoustic system, the vibratory behavior of the structure is assumed to be known from modal analysis or from experiment, and the radiative energy transfer method is involved for high-frequency acoustical studies. The main equations of this method are exposed in Section 1, and the hybrid method is presented in Section 2. Section 3 is dedicated to numerical and experimental validations of the approach in the case of a free ribbed rectangular plate sandwiched between two absorbant panels.

2. Radiative energy transfer equations

2.1. General form of the equations for three-dimensional systems

The radiative energy transfer method is a ray method which relies on an integral equation on energy. It is particularly well-suited for high-frequency applications and has already been successfully applied to the structure–acoustic coupling above the critical frequency for plane structures [21] and to the determination of SPL in rooms [22]. Further developments are also proposed in other energy methods dedicated to room acoustics [23]. This method is based on energy local quantities which are the energy density W and the intensity $\mathbf{I}$. Three assumptions are necessary to derive the energy model: the acoustical medium is assumed to be isotropic and homogeneous, evanescent and near-field waves are neglected, and finally, interferences between propagative waves are neglected. In this method, energy fields are considered as the superposition of actual and fictitious sources [24]. With only surface sources of power σ ($\mathrm{W/m^2}$) located at $\mathbf{p}$ on the surface Γ, the energy density at any receiver point $\mathbf{r}$ inside the domain Ω is expressed as

$$W(\mathbf{r}) = \int_{\Gamma} \sigma(\mathbf{p},\mathbf{u}) G(\mathbf{p},\mathbf{r})\, \mathrm{d}\Gamma \tag{1}$$

and the corresponding intensity is

$$\mathbf{I}(\mathbf{r}) = \int_{\Gamma} \sigma(\mathbf{p},\mathbf{u}) \mathbf{H}(\mathbf{p},\mathbf{r})\, \mathrm{d}\Gamma, \tag{2}$$

where $\mathbf{u}$ is the unit vector from the source point $\mathbf{p}$ to the receiver point $\mathbf{r}$. G and $\mathbf{H}$ are the kernel functions for energy quantities

$$G(\mathbf{s},\mathbf{r}) = \frac{\mathrm{e}^{-mr}}{4\pi c r^2}, \tag{3}$$

c is the speed of sound, m is the atmospheric attenuation factor, and $r = |\mathbf{r} - \mathbf{s}|$ is the source–receiver distance. The kernel function $\mathbf{H}$ for intensity can be related to the kernel function G for energy density by a proportionality relationship valid for propagative waves,

$$\mathbf{H}(\mathbf{s},\mathbf{r}) = cG(\mathbf{s},\mathbf{r})\mathbf{u}. \tag{4}$$

The fields W and $\mathbf{I}$ respect the local power balance in steady-state conditions. Eqs. (1) and (2) are the fundamental integral equations of the radiative energy transfer method for three-dimensional systems.

2.2. Source partitioning for the hybrid method

In the scope of the proposed hybrid method, the surface sources are divided into two contributions which are, respectively, called equivalent and fictitious sources. The equivalent sources are introduced on the surface S of the vibrating structure to reproduce its acoustical radiation behavior. The fictitious sources depend on the acoustical environment of the structure and are introduced on the overall domain boundary Γ including the surface S itself to model phenomena such as reflection and eventually diffraction. The energy density at any receiver point $\mathbf{r}$ is therefore the sum of two contributions, one coming from the equivalent sources of power σ_e ($\mathrm{W/m^2}$) located at $\mathbf{q}$ on S, and one coming from the fictitious sources of power σ_f ($\mathrm{W/m^2}$) located at $\mathbf{p}$ on Γ (Fig. 1),

$$W(\mathbf{r}) = \int_S \sigma_e(\mathbf{q},\mathbf{u})G(\mathbf{q},\mathbf{r})\,\mathrm{d}S + \int_\Gamma \sigma_f(\mathbf{p},\mathbf{u})G(\mathbf{p},\mathbf{r})\,\mathrm{d}\Gamma \tag{5}$$

and the corresponding intensity is

$$\mathbf{I}(\mathbf{r}) = \int_S \sigma_e(\mathbf{q},\mathbf{u})\mathbf{H}(\mathbf{q},\mathbf{r})\,\mathrm{d}S + \int_\Gamma \sigma_f(\mathbf{p},\mathbf{u})\mathbf{H}(\mathbf{p},\mathbf{r})\,\mathrm{d}\Gamma. \tag{6}$$

Eqs. (5) and (6) are the fundamental integral equations of the hybrid method based on the radiative energy transfer method. The hybrid method can be divided into three steps to compute the equivalent sources σ_e, then the fictitious sources σ_f, and finally the acoustical field. Fig. 2 is a schematic illustration of these steps which are described in the following sections.

3. Introduction of equivalent energy sources

The key point of the hybrid method is to approximate the vibratory field by a set of equivalent acoustical sources which are intended to reproduce the far-field radiated noise (Fig. 2(a)). These sources depend on the surface vibrational velocity.

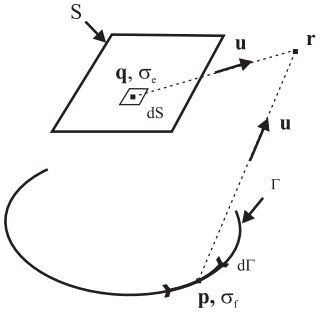

Fig. 1. Source partitioning for the hybrid method: the acoustical field at point $\mathbf{r}$ is given by superimposing the contribution from the equivalent sources σ_e at $\mathbf{q}$ on S and the contribution from the fictitious sources σ_f at $\mathbf{p}$ on Γ.

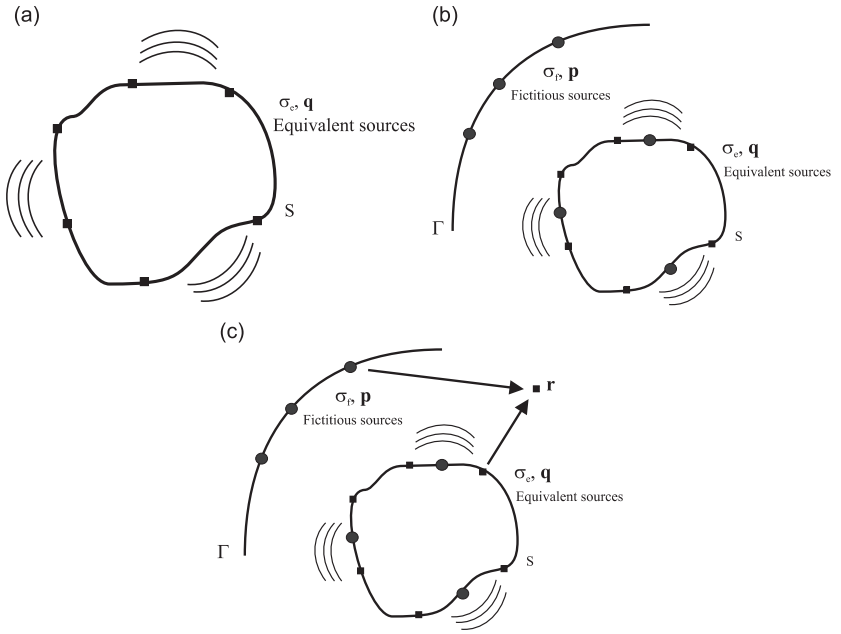

Fig. 2. The three steps of the hybrid method: (a) the first step is the computation of equivalent sources σ_e introduced at $\mathbf{q}$ on the vibrating surface S intended to reproduce its free field radiation; (b) the second step is the computation of fictitious sources σ_f introduced at $\mathbf{p}$ on the domain boundary Γ (including S) to model phenomena such as reflection; and (c) the third and last step is the computation of the acoustical field at point $\mathbf{r}$ by summing all the source contributions.

3.1. Amplitude of the equivalent sources

In the decomposition of Eqs. (5) and (6), the term σ_f includes all the effects due to reflection and diffraction of rays hitting the surface at $\mathbf{p}$. So, the evaluation of the radiation term σ_e can be done by eliminating the remote obstacles or, in other words, by considering the structure S as if radiating in the free field.

3.1.1. Acoustical energy radiated in the free field

The noise radiated by an arbitrary vibrating structure is given by the Helmholtz–Kirchhoff integral equation which relates the normal acceleration γ_n at point $\mathbf{q}$ on the surface S of the structure to the radiated sound pressure field p at any receiver point $\mathbf{r}$ in the surrounding acoustical fluid [25],

$$p(\mathbf{r}) = \int_S \rho_0 \gamma_n(\mathbf{q}) g(\mathbf{q},\mathbf{r}) + p(\mathbf{q}) \frac{\partial g(\mathbf{q},\mathbf{r})}{\partial n}\, \mathrm{d}S. \tag{7}$$

ρ_0 denotes the fluid density, $\partial/\partial n$ means the derivative in the direction of the outward normal $\mathbf{n_q}$ at point $\mathbf{q}$. $g(\mathbf{q},\mathbf{r}) = \mathrm{e}^{-\mathrm{j}kr}/4\pi r$ is the free field Green's function, $r = |\mathbf{r}-\mathbf{q}|$ is the source–receiver distance and k is the complex wavenumber expressed as $k = k_0 - \mathrm{j}m/2$ where $k_0 = \omega/c$. The time-averaged acoustic energy density W is

$$W(\mathbf{r}) = \frac{|p(\mathbf{r})|^2}{2\rho_0 c^2}. \tag{8}$$

Thus, introducing Eq. (7) into Eq. (8), the energy density is given by

$$\begin{aligned} W(\mathbf{r}) = & \int\int_{S\times S} \frac{1}{2\rho_0 c^2} p(\mathbf{q}) p^*(\mathbf{q}') \frac{\partial g(\mathbf{q},\mathbf{r})}{\partial n} \frac{\partial g^*(\mathbf{q}',\mathbf{r})}{\partial n}\, \mathrm{d}S'\, \mathrm{d}S \\ & + \int\int_{S\times S} \frac{\rho_0}{2c^2} \gamma_n(\mathbf{q})\, \gamma_n^*(\mathbf{q}') g(\mathbf{q},\mathbf{r})\, g^*(\mathbf{q}',\mathbf{r})\, \mathrm{d}S'\, \mathrm{d}S \\ & + \mathrm{Re}\left(\int\int_{S\times S} \frac{1}{c^2} \gamma_n(\mathbf{q}) p^*(\mathbf{q}') g(\mathbf{q},\mathbf{r}) \frac{\partial g^*(\mathbf{q}',\mathbf{r})}{\partial n}\, \mathrm{d}S'\, \mathrm{d}S \right), \end{aligned} \tag{9}$$

where * denotes the conjugate quantity.

3.1.2. Ensemble averaging

The transition from low frequencies to high frequencies requires to remove all the microscopic details of the evolution of the energy in Eq. (9). These details are irrelevant for a macroscopic prediction and can be considered as unpredictable. This is done by introducing an ensemble average operator (denoted $\langle\cdot\rangle$). Ensemble averaging is justified by the fact that the vibroacoustic behavior of a system varies because of the inherent uncertainties on physical and geometrical properties, all the more as the frequency increases. Thus, ensemble averaging is commonly used in high-frequency methods, as in the EBEA [13] where, in addition, only the cross-products taken at the same point are non-zero. Viktorovitch [3,4] introduces randomness in the geometrical description of the structure. In this study, the surface pressure and acceleration fields are considered as random variables. The randomness is introduced in the phase of these quantities. Under this assumption, the Green's functions are determinist functions. The far-field approximation is used stating that $kr \gg 1$, and the difference between r and r' is assumed to be small enough so that $r \simeq r'$ and thus $m/2(r+r') \simeq mr$. It follows that the cross-products involving the Green's functions can be simplified (Appendix A). Finally, under these conditions and noting that $\langle W\rangle$ is a real quantity, three kinds of boundary sources with amplitudes σ_{pp}, $\sigma_{\gamma\gamma}$ and $\sigma_{p\gamma}$ are found: these sources are, respectively, called pressure source, velocity source and intensity source. The acoustic energy density due to their contributions is

$$\langle W(\mathbf{r})\rangle = \int_S (\sigma_{pp}(\mathbf{q},\mathbf{r}) + \sigma_{\gamma\gamma}(\mathbf{q},\mathbf{r}) + \sigma_{\gamma p}(\mathbf{q},\mathbf{r}))\, G(\mathbf{q},\mathbf{r})\, \mathrm{d}S, \tag{10}$$

with

$$\sigma_{pp}(\mathbf{q},\mathbf{r}) = \mathrm{Re}\left(\frac{k^2}{8\pi\rho_0 c} r \mathrm{e}^{-\mathrm{j}k_0 r}\, (\mathbf{u}\cdot\mathbf{n}_\mathbf{q}) \int_S R_{pp}(\mathbf{q},\mathbf{q}') \frac{\mathrm{e}^{\mathrm{j}k_0 r'}}{r'} (\mathbf{u}'\cdot\mathbf{n}_{\mathbf{q}'})\, \mathrm{d}S'\right), \tag{11}$$

$$\sigma_{\gamma\gamma}(\mathbf{q},\mathbf{r}) = \mathrm{Re}\left(\frac{\rho_0}{8\pi c} r \mathrm{e}^{-\mathrm{j}k_0 r} \int_S R_{\gamma\gamma}(\mathbf{q},\mathbf{q}') \frac{\mathrm{e}^{\mathrm{j}k_0 r'}}{r'}\, \mathrm{d}S'\right), \tag{12}$$

$$\sigma_{\gamma p}(\mathbf{q},\mathbf{r}) = \mathrm{Re}\left(\frac{-\mathrm{j}k^*}{4\pi c} r \mathrm{e}^{-\mathrm{j}k_0 r} \int_S R_{\gamma p}(\mathbf{q},\mathbf{q}') \frac{\mathrm{e}^{\mathrm{j}k_0 r'}}{r'} (\mathbf{u}'\cdot\mathbf{n}_{\mathbf{q}'})\, \mathrm{d}S'\right). \tag{13}$$

$\mathbf{n}_\mathbf{q}$ (respectively $\mathbf{n}_{\mathbf{q}'}$) is the unit outward normal to the surface of the structure at point $\mathbf{q}$ (respectively $\mathbf{q}'$). $\mathbf{u}$ (respectively $\mathbf{u}'$) is the unit vector from the source point $\mathbf{q}$ (respectively $\mathbf{q}'$) to the receiver point $\mathbf{r}$. $R_{pp}(\mathbf{q},\mathbf{q}') = \langle p(\mathbf{q}) p^*(\mathbf{q}')\rangle$, $R_{\gamma\gamma}(\mathbf{q},\mathbf{q}') = \langle \gamma_n(\mathbf{q}) \gamma_n^*(\mathbf{q}')\rangle$, and $R_{\gamma p}(\mathbf{q},\mathbf{q}') = \langle \gamma_n(\mathbf{q}) p^*(\mathbf{q}')\rangle$ are the pressure, acceleration and intensity cross-spectral densities, that is the cross-correlation of two fields at points $\mathbf{q}$ and $\mathbf{q}'$. These equivalent sources are related to those introduced in the integral equation for frequency averaged quadratic pressure [5–8], except that the cross-products between Green's functions are evaluated as frequency averages in the integral equation rather than ensemble averages of determinist quantities. Despite all, frequency averaging is often considered as equivalent to ensemble averaging such that, under this consideration, the equivalent sources as developed until now are similar to those introduced in the frequency averaged quadratic pressure method. Compared to the simplified BEM [9–11], and to the EBEA [12,13], the cross-contributions between surface fields taken at different points are not neglected as they represent the interactions between the surface sources that lead to short-circuit effects and edge, corner and surface modes.

3.1.3. Ray approximation

At this stage, the strengths of the equivalent sources (Eqs. (11)–(13)) depend both on the source position $\mathbf{q}$ on the vibrating surface and on the position of the receiver point $\mathbf{r}$. This is not in agreement with the assumptions used in the radiative energy transfer method. Indeed, the radiative energy transfer method is a ray method [22] which follows the geometrical acoustic laws. It is shown in Appendix B that the principle of energy conservation inside a ray tube requires that the strength of a source involved in the radiative energy transfer method be the same along a ray and thus only depend on the direction of emission. To introduce equivalent sources which respect this condition, the difference of acoustical way $r - r'$ is estimated in the far

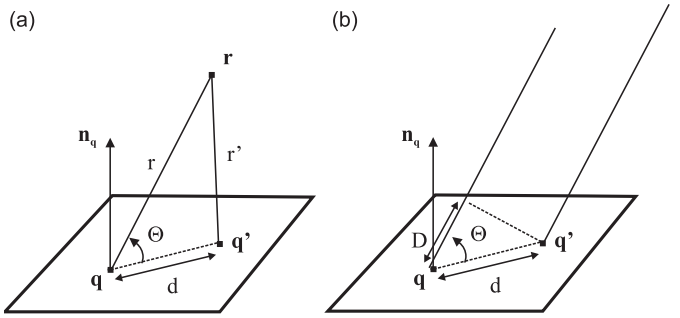

Fig. 3. (a) For ray approximation, the difference of acoustical way r–r' between $\mathbf{q}$ and $\mathbf{q}'$ is estimated in the far field: $d = |\mathbf{q}' - \mathbf{q}|$ is the distance between the source points $\mathbf{q}$ and $\mathbf{q}'$ and Θ is the emission angle from the source point $\mathbf{q}$; (b) the relation obtained $D = d\cos\Theta$ is equivalent to the one obtained when plane waves are emitted at points $\mathbf{q}$ and $\mathbf{q}'$.

field. The distance from the source point $\mathbf{q}$ to the receiver point $\mathbf{r}$ is given by (Fig. 3(a))

$$r'^2 = r^2 + d^2 - 2rd\cos\Theta, \tag{14}$$

where $d = |\mathbf{q}' - \mathbf{q}|$ is the distance between the source points $\mathbf{q}$ and $\mathbf{q}'$ and Θ is the emission angle from the source point $\mathbf{q}$. In the far field, $r \gg d$, thus the above relationship can be simplified to

$$r' \simeq r - d\cos\Theta. \tag{15}$$

This relation is strictly similar to the one obtained under the assumption that plane waves are emitted at points $\mathbf{q}$ and $\mathbf{q}'$ (Fig. 3(b)). Finally, in the far field $r \simeq r'$ and the amplitudes σ_{pp}, $\sigma_{\gamma\gamma}$ and $\sigma_{p\gamma}$ can be written as

$$\sigma_{pp}(\mathbf{q},\mathbf{u}) = \mathrm{Re}\left(\frac{k^2}{8\pi\rho_0 c}(\mathbf{u}\cdot\mathbf{n}_\mathbf{q})^2 \int_S R_{pp}(\mathbf{q},\mathbf{q}')\mathrm{e}^{-\mathrm{j}k_0 d\cos\Theta}\,\mathrm{d}S'\right), \tag{16}$$

$$\sigma_{\gamma\gamma}(\mathbf{q},\mathbf{u}) = \mathrm{Re}\left(\frac{\rho_0}{8\pi c}\int_S R_{\gamma\gamma}(\mathbf{q},\mathbf{q}')\mathrm{e}^{-\mathrm{j}k_0 d\cos\Theta}\,\mathrm{d}S'\right), \tag{17}$$

$$\sigma_{\gamma p}(\mathbf{q},\mathbf{u}) = \mathrm{Re}\left(\frac{-\mathrm{j}k^*}{4\pi c}(\mathbf{u}\cdot\mathbf{n}_\mathbf{q})\int_S R_{\gamma p}(\mathbf{q},\mathbf{q}')\mathrm{e}^{-\mathrm{j}k_0 d\cos\Theta}\,\mathrm{d}S'\right). \tag{18}$$

Thus modified, the amplitudes of the equivalent sources only depend on the direction of emision $\mathbf{u}$, and more precisely they depend on the angle θ between the direction $\mathbf{u}$ and the outward normal $\mathbf{n}_\mathbf{q}$ at the source position $\mathbf{q}$. These sources are adapted to the implementation of the radiative energy transfer method whereby they are introduced as actual sources on the surface of the vibrating structure.

3.2. Evaluation of the surface fields

Explicit expressions for the equivalent sources are presented in Eqs. (16)–(18). These sources depend not only on the surface velocity field but also on the pressure surface field which is assumed to be unknown. This problem is the same as in the BEM where the pressure at any field point is obtained from the surface pressure and normal velocity by fieldpoint postprocessing. As discussed in the Introduction, the calculation of these surface fields is the most expensive in terms of CPU time because it involves the inversion of a fully populated matrix. In the same way, two boundary integral equations are derived in the BEM based on energy quantities [5–11] where only the FACV source is known, and it is necessary to relate the FACP and the FACI sources to this one.

In the case of the hybrid method, the strategy to adopt to estimate the pressure surface field depends on how the velocity field is obtained. If this field is issued from experiments, a method such as the two-microphone

method allows to measure simultaneously both the surface pressure and velocity fields. If this field is issued from numerical calculations or from velocity measurements, it is suggested to apply the Kirchhoff–Helmholtz equation on the domain boundary, that is the same first step as in the BEM. Let keep in mind that only the vibrating structure as if radiating in an unbounded medium should be discretized and so the number of mesh elements is far less than in the complete BEM where it is also necessary to mesh the acoustical environment of this structure.

3.3. Physical interpretation of the equivalent sources

The amplitudes of the equivalent sources can be related to the normal intensity on the surface of the vibrating structure. Let consider a sphere S_ε of radius ε surrounding the source point $\mathbf{q}$. The power $\mathrm{d}P_{\mathrm{emit}}$ emitted by an infinitesimal surface $\mathrm{d}S$ surrounding $\mathbf{q}$ is the flux of intensity due to the source $\sigma_e(\mathbf{q},\mathbf{u})\,\mathrm{d}S$ through a part of the sphere $\mathrm{d}S_\varepsilon = \varepsilon^2 \mathrm{d}\alpha$,

$$\begin{aligned}\mathrm{d}P_{\mathrm{emit}} &= \int_{S_\varepsilon} \mathrm{d}\mathbf{I}(\mathbf{q}) \cdot \mathrm{d}\mathbf{S}_\varepsilon \\ &= \int_{S_\varepsilon} \sigma_e(\mathbf{q},\mathbf{u})\,\mathrm{d}S \frac{\mathrm{e}^{-m\varepsilon}}{4\pi\varepsilon^2}\,\mathrm{d}S_\varepsilon \\ &= \frac{\mathrm{e}^{-m\varepsilon}}{4\pi}\,\mathrm{d}S \int_A \sigma_e(\mathbf{q},\mathbf{u})\,\mathrm{d}\alpha. \end{aligned} \tag{19}$$

$\mathrm{d}\alpha$ and A, respectively, denote the infinitesimal and the total solid angle of emission. Taking the limit for small ε,

$$\mathrm{d}P_{\mathrm{emit}} = \frac{1}{4\pi}\,\mathrm{d}S \int_A \sigma_e(\mathbf{q},\mathbf{u})\,\mathrm{d}\alpha. \tag{20}$$

Now, the power emitted by the infinitesimal surface $\mathrm{d}S$ surrounding $\mathbf{q}$ can also be written by means of the normal intensity I_n at point $\mathbf{q}$ as

$$\mathrm{d}P_{\mathrm{emit}} = \langle I_n(\mathbf{q})\rangle \mathrm{d}S. \tag{21}$$

Finally, the following relation between the amplitudes of the equivalent sources and the normal intensity on the surface of the vibrating structure can be established:

$$\langle I_n(\mathbf{q})\rangle = \frac{1}{4\pi}\int_A \sigma_e(\mathbf{q},\mathbf{u})\,\mathrm{d}\alpha, \tag{22}$$

where the integral is performed over all the directions of emission $\mathbf{u}$.

4. Introduction of fictitious energy sources

Once the equivalent sources known, the vibrating structure is not considered anymore as if radiating in an unbounded medium but the acoustical environment of the structure is taken into account. Fictitious sources are introduced on the domain boundary where acoustical phenomena such as reflection or absorption occur (Fig. 2(b)). Note that the domain boundary includes the vibrating structure itself and so fictitious sources are also introduced on its surface. These sources are the new unknowns to determine, and they are predicted using the radiative energy transfer equations given in Eqs. (1) and (2). The fictitious sources are assumed to follow the Lambert's law so that their amplitude σ_f can be written as

$$\sigma_f(\mathbf{p},\mathbf{u}) = \sigma_f(\mathbf{p})\cos\theta, \tag{23}$$

where θ is the angle between the direction of emission $\mathbf{u}$ and the outward normal $\mathbf{n_p}$ to the fluid domain at point $\mathbf{p}$. The equation over σ_f is obtained by applying the power balance on the domain boundary Γ. In the case of an absorbing boundary with absorption coefficient α, the relation between the emitted power and the incident power has the form

$$\mathrm{d}P_{\mathrm{emit}} = (1-\alpha)\,\mathrm{d}P_{\mathrm{inc}}. \tag{24}$$

Let first consider the power emitted by the fictitious source at point **p**. As discussed in Eq. (20), the power emitted by an infinitesimal surface $\mathrm{d}\Gamma$ surrounding **p** has the form

$$\begin{aligned} \mathrm{d}P_{\mathrm{emit}} &= \frac{1}{4\pi}\,\mathrm{d}\Gamma \int_A \sigma_f(\mathbf{p},\mathbf{u})\,\mathrm{d}\alpha \\ &= \frac{1}{4\pi}\,\sigma_f(\mathbf{p})\,\mathrm{d}\Gamma \int_A \cos\theta\,\mathrm{d}\alpha \\ &= \frac{\sigma_f(\mathbf{p})}{4}\,\mathrm{d}\Gamma. \end{aligned} \tag{25}$$

Then, the incident power comes both from the equivalent sources σ_e located at **q** emitting in the direction **u** towards **p**, and from the other fictitious sources σ_f located at $\mathbf{p}'$ emitting in the direction $\mathbf{u}'$ towards **p** (Fig. 4). Each contribution is expressed as the flux of energy flow over the infinitesimal surface $\mathrm{d}\Gamma$,

$$\begin{aligned} \mathrm{d}P_{\mathrm{inc}} = &\int_S \sigma_e(\mathbf{q},\mathbf{u})\mathbf{H}(\mathbf{q},\mathbf{p})\cdot\mathbf{n}_{\mathbf{p}}\,\mathrm{d}S\,\mathrm{d}\Gamma \\ &+ \int_\Gamma \sigma_f(\mathbf{p}')\cos\theta'\mathbf{H}(\mathbf{q}',\mathbf{p})\cdot\mathbf{n}_{\mathbf{p}}\,\mathrm{d}\Gamma'\,\mathrm{d}\Gamma. \end{aligned} \tag{26}$$

θ' is the angle between the direction of emission $\mathbf{u}'$ and the outward normal $\mathbf{n}_{\mathbf{p}'}$ to the fluid domain at point $\mathbf{p}'$. Finally, using Eq. (24), the equation over the unknowns σ_f is given by

$$\begin{aligned} \frac{\sigma_f(\mathbf{p})}{4} = &(1-\alpha)\int_S \sigma_e(\mathbf{q},\mathbf{u})\mathbf{H}(\mathbf{q},\mathbf{p})\cdot\mathbf{n}_{\mathbf{p}}\,\mathrm{d}S \\ &+ (1-\alpha)\int_\Gamma \sigma_f(\mathbf{p}')\cos\theta'\,\mathbf{H}(\mathbf{p}',\mathbf{p})\cdot\mathbf{n}_{\mathbf{p}}\,\mathrm{d}\Gamma'. \end{aligned} \tag{27}$$

This equation can be related to the one introduced in Ref. [22]: the difference is that the real sources introduced in the hybrid method are the equivalent sources σ_e which are surface and not volumic sources. Other equations are derived in cases of diffuse or specular reflection [26], or in the case of diffraction [27]. Eq. (27) relates the fictitious sources σ_f to the equivalent sources σ_e whose formulations involve the velocity field generally provided by a low-frequency structural approach. Hence, the equivalent sources described in the hybrid method proposed allow to apply a high-frequency energy method from data originated from a low-frequency method. The contributions of the fictitious sources are added to the contributions of the equivalent sources to compute the acoustical field around a structure vibrating in any acoustical environment using Eqs. (5) and (6) (Fig. 2(c)).

5. Example application: noise radiated by a ribbed free plate

The proposed method is illustrated by application to the case of a ribbed plate. The plate is made with cast aluminium and its dimensions are 400 mm length, 230 mm width, 10 mm thick at the ribs and 5 mm thick

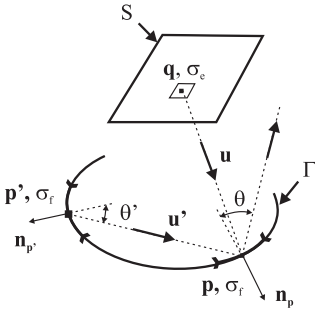

Fig. 4. Power balance at the fictitious source point **p**: the incident power comes from the equivalent sources at point **q** emitting in the direction **u** towards **p** and from the other fictitious sources at point $\mathbf{p}'$ emitting in the direction $\mathbf{u}'$ towards **p**.

everywhere else (Fig. 5(a)). The plate is sandwiched between two absorbant panels (Fig. 5(b)) made with foams of thickness 25 mm for the upper panel and 50 mm for the lower panel. The absorption coefficients are given in Table 1. The hybrid method is applied to predict the noise radiated by the plate at two field points in the surrounding environment. Firstly, equivalent sources are introduced on the surface of the plate and evaluated from the surface pressure and velocity fields which are measured using the two-microphone technique for this application. Secondly, fictitious sources located on the boundary of the acoustical domain are computed using the radiative energy transfer method. Thirdly and finally, the acoustical field at the two points is given by summing the contributions of all these sources and the result thus simulated is compared to a reference one. These points are detailed in the following sections.

5.1. Pressure and velocity measurements on the surface of the ribbed plate

Experimental measurements are made to evaluate surface velocity and pressure fields. The sound pressure field is scanned over two parallel planes with a $1/4''$ microphone receiver. This task is realized experimentally thanks to a robotic scanning facility system which allows to move the microphone along the three coordinates axis. A surface accelerometer located at $x = 20$ mm and $y = 225$ mm from the right top corner of the plate gives the reference signal for phase measurements. Data from the microphone and from the accelerometer are collected with a FFT analyzer connected to a computer which provides the data recording. The ribbed plate is suspended to a frame approximating free boundary conditions. The experiment consists in driving a shaker located behind the plate with a white noise in a bandwith from 0 to 5 kHz. The computer did record the power spectrum from the microphone and from the accelerometer, as well as the real and imaginary part of the transfer function between pressure and acceleration for 201 equispaced frequencies on the whole frequency band, which means a resolution of 25 Hz. Two measurement planes are chosen so that the particle velocity

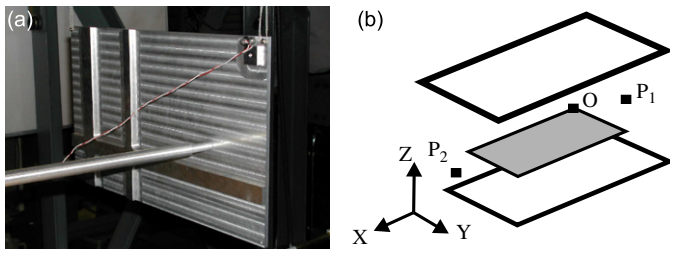

Fig. 5. (a) Ribbed plate used for the experiments; (b) for numerical simulations, the plate is sandwiched between two absorbant panels.

Table 1
Absorption coefficient versus frequency

Octave band (Hz)	Absorption coefficient
(a) For the upper absorbant panel made with foam of thickness 25 mm	
125	0.14
250	0.30
500	0.63
1000	0.91
2000	0.98
4000	0.91
(b) For the lower panel made with foam of thickness 50 mm [28]	
125	0.35
250	0.51
500	0.82
1000	0.98
2000	0.97
4000	0.95

midway between them can be calculated. The distance between the plate and the first measurement plane is 10 mm and the distance between the two measurement planes is 10 mm. These distance are small enough to consider that surface fields are measured by this way. Both measurement planes are centered on the center of the plate. The microphone is positioned at the first point in the left bottom corner of the first plane parallel to the plate. Data are saved and the microphone is moved perpendicularly to the plate so that data on the second measurement plane be saved. Proceeding the same way, the microphone is moved vertically taking data every 10 mm along the first line for both measurement planes. When the microphone has completed a vertical line, it is moved parallel to the plate and a second vertical scan is performed. The spacing between measurement points is always 10 mm which is suitable for measurements up to 5 kHz according to the criteria of 6 elements per wavelength.

The measurement of the pressure field on two parallel closely spaced planes allows to compute the gradient, and then the particle velocity. The sound pressure on the two measurement planes is given by

$$p_1(t) = p_1 e^{j(\omega t+\phi_1)}, \tag{28}$$

$$p_2(t) = p_2 e^{j(\omega t+\phi_2)}, \tag{29}$$

where p_1 and p_2 are the pressure amplitudes and ϕ_1 and ϕ_2 are the pressure phases, respectively, on the first and the second measurement plane. ω is the angular frequency. The pressure midway between the measurement planes is given by

$$p(t) = \frac{(p_1(t) + p_2(t))}{2} \tag{30}$$

and the particle velocity midway between the measurement planes is given by

$$u(t) = u e^{j(\omega t+\phi_u)}, \tag{31}$$

$$u = \frac{1}{\rho_0 \Delta r \omega} \sqrt{p_1^2 + p_2^2 - 2p_1 p_2 \cos(\phi_1 - \phi_2)} \tag{32}$$

$$\phi_u = \arg((p_1 \sin\phi_1 - p_2 \sin\phi_2) + j(p_2 \cos\phi_2 - p_1 \cos\phi_1)), \tag{33}$$

where ρ_0 is the density of air and Δr is the distance between the measurement planes. The maps presented on Fig. 6 show the pressure (a) and the velocity (b) fields measured over the plate at 2500 Hz.

5.2. The equivalent sources

The first step of the hybrid method is to introduce equivalent sources intended to reproduce the noise radiated by the vibrating structure that is the plate in this application. For that purpose, only the plate is firstly taken into account without its acoustical environment. Each equivalent source is the sum of three

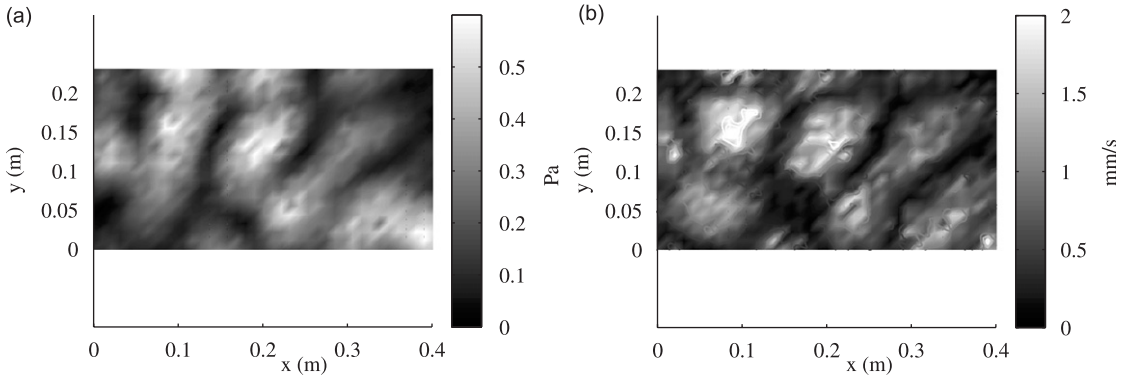

Fig. 6. (a) Pressure in Pa and (b) velocity in mm/s measured by the two-microphone method on the ribbed plate surface. The frequency is 2500 Hz.

contributions corresponding respectively to a pressure source, a velocity source and an intensity source. The amplitude and directivity are evaluated using Eqs. (16)–(18) from the measured surface fields. For this purpose, the cross-products between surface fields that are experimentally obtained every 25 Hz from 0 to 5 kHz are frequency-averaged within each frequency band. For instance, for the third-octave centered on 2500 Hz with lower frequency limit 2250 Hz and upper frequency limit 2800 Hz, ensemble averaging is performed over 23 data sets. The noise radiated in the free field by the plate is given by superimposing the contributions of the equivalent sources. To check the validity of these sources, the result thus obtained is compared to the BEM result for two configurations. Comparisons are carried out on a line perpendicular to the plate depicted on Fig. 7(a), and on a half-sphere of radius 3 m centered on the center of the plate. Calculations are carried out on the third-octave band centered on 2500 Hz: BEM results that are obtained at pure tone frequencies every 10 Hz between 2250 Hz and 2800 Hz are frequency-averaged within this band while analysis with the equivalent sources are performed at the central frequency of the band. Figs. 7(b) and 8, respectively, present the SPL along the line and the maps of the SPL on the half-sphere computed from the equivalent sources and from the BEM. Results obtained with the two numerical methods are very similar. Besides, the directivity characteristics of the radiated field are well reproduced.

5.3. *The fictitious sources*

The equivalent sources are now used to compute the acoustical field around the vibrating structure in any environment. This is the second step of the hybrid method. Fictitious sources are introduced on the domain boundary, that is the absorbant panels and the plate itself which is a perfectly reflecting surface. The amplitudes of these sources are derived from the radiative transfer energy equations. The SPL is computed at two points between the absorbant panels located at $(-1.6, 0.2, 0.1)$ m, $(2, 0.2, 0.1)$ m in the frame of the plate (Fig. 5(b)). BEM results are used as a reference to check the validity of the method. Calculations are carried out on four octave bands respectively centered on 500, 1000, 2000 and 4000 Hz: in the same way as previously, BEM results that are obtained at pure tone frequency every 50 Hz are frequency-averaged within each band while analysis with the radiative transfer energy method are performed at the central frequency of the band. The number of elements in the BEM model is chosen to check the conventional criteria of 6 elements per wavelength which leads to about 5000 elements, and the number of elements for the radiative transfer energy method is about 200. Computed results are shown in Fig. 9. The proposed method leads to a large 15 dB error on the lower frequency band. Indeed, the number of modes on this frequency band is not high enough to be in the high-frequency range and thus the proposed method is not valid. For the upper frequency bands, good

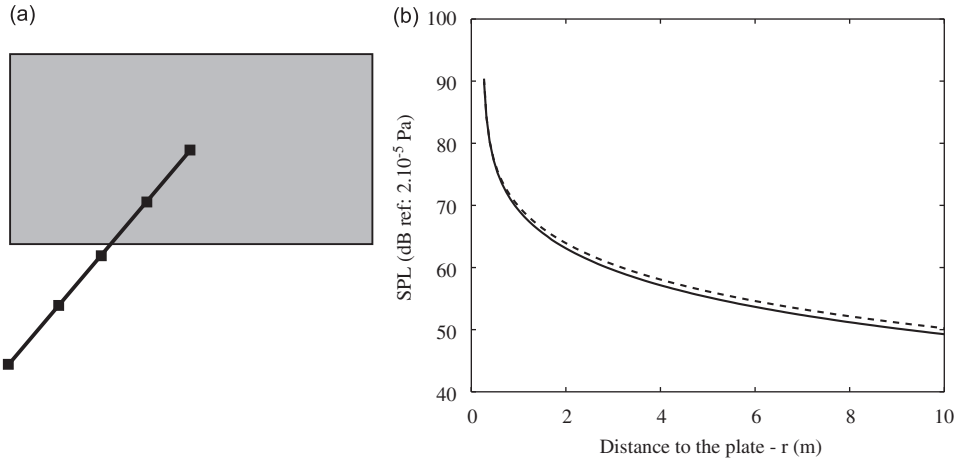

Fig. 7. (a) Calculations of the sound pressure level along a line from the center of the ribbed plate when vibrating in free field; (b) comparison of the sound pressure level in dB (ref: 2×10^{-5} Pa) along the line computed with the BEM (−−) and with the equivalent sources (——). Calculations are carried out on the third-octave band centered on 2500 Hz.

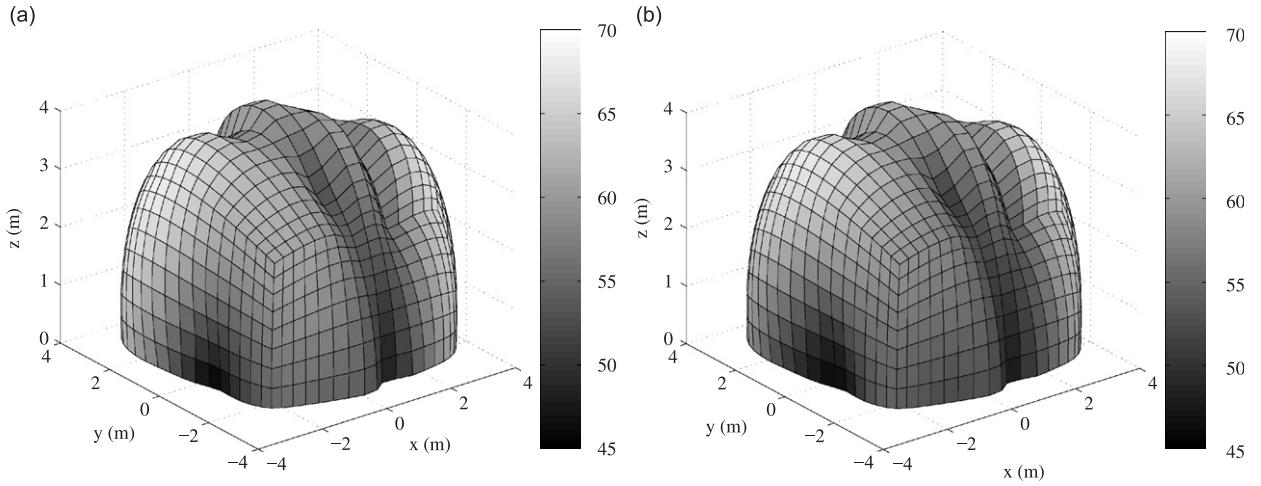

Fig. 8. Sound pressure level in dB (ref: 2×10^{-5} Pa) on a half-sphere of radius 3 m surrounding the ribbed plate when vibrating in free field, computed (a) with the BEM and (b) with the equivalent sources. Calculations are carried out on the third-octave band centered on 2500 Hz.

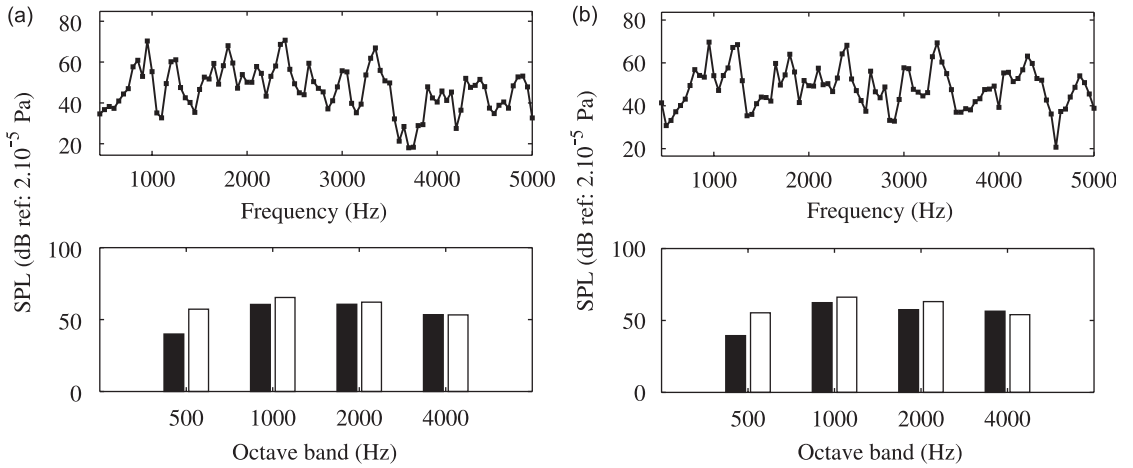

Fig. 9. Sound pressure level in dB (ref: 2×10^{-5} Pa) (a) at point $(-1.6, 0.2, 0.1)$ m and (b) at point $(2, 0.2, 0.1)$ m in the plate frame: the upper curve presents the BEM result at pure tone frequency every 50 Hz between 350 and 5650 Hz, the lower curve compares the BEM result frequency-averaged on octave band (■) to the hybrid result (□) for 4 octave bands respectively centered on 500, 1000, 2000 and 4000 Hz.

agreement between the two methods is observed. The computation times on a 2.53 GHz Pentium 4 are, respectively, about 10 s for calculations at the two points and on one octave band with the energy method, and about 20 min for calculations at the two points and at a fixed frequency with the BEM. Thus computation times are seriously reduced, all the more as only one calculation over each frequency band is carried out with the energy method.

6. Conclusion

A method is proposed to predict the noise radiated by a vibrating structure in the high-frequency range using the radiative energy transfer method. Equivalent energy sources well suited for the implementation of the method are introduced on the surface of the structure. The amplitudes of these energy sources depend both

on the source position and on the direction of emission. Analytical formulations involving the cross-spectral densities of the surface fields are derived from the computation of the ensemble average of the acoustical energy density. Thus, three kinds of equivalent sources, respectively, called pressure, velocity and intensity sources are introduced. Once these equivalent sources known, the noise radiated by a vibrating structure with any acoustical environment such as an open or a closed enclosure can be predicted using the radiative energy transfer method. The main interest of the radiative energy transfer method is that calculations are performed on frequency bands and with quite a coarser mesh compared to classical methods based on finite elements such that computational times are seriously reduced. Finally, the hybrid method appears as a tool to couple any approach providing the vibratory behavior of a structure to the radiative energy transfer method to predict the noise radiated in the high-frequency range.

Acknowledgments

The authors acknowledge the French Centre National de la Recherche Scientifique and the financial support by the Japan Society for Promotion of Science to carry out experiments in Japan.

Appendix A

This appendix details the formulations of the cross-products involving the Green's function as obtained to get Eqs. (11)–(13). The Green's function is given by

$$g(\mathbf{q},\mathbf{r}) = \frac{\mathrm{e}^{-\mathrm{j}kr}}{4\pi r} \tag{A.1}$$

and its normal derivative

$$\frac{\partial g(\mathbf{q},\mathbf{r})}{\partial n} = -\left(\mathrm{j}k + \frac{1}{r}\right)\frac{\mathrm{e}^{-\mathrm{j}kr}}{4\pi r}\frac{\partial r}{\partial n}, \tag{A.2}$$

where

$$\frac{\partial r}{\partial n} = \mathbf{u}\cdot\mathbf{n}_{\mathbf{q}}. \tag{A.3}$$

Under these considerations, the cross-products $g\cdot g^*$, $\partial g/\partial n\cdot\partial g^*/\partial n$ and $g\cdot\partial g^*/\partial n$ are, respectively, written as

$$\begin{aligned} g(\mathbf{q},\mathbf{r})g^*(\mathbf{q}',\mathbf{r}) &= \frac{\mathrm{e}^{-\mathrm{j}(kr-k^*r')}}{16\pi^2 rr'} \\ &= \frac{\mathrm{e}^{-\mathrm{j}k_0(r-r')}\mathrm{e}^{-m/2(r+r')}}{16\pi^2 rr'}, \end{aligned} \tag{A.4}$$

$$\begin{aligned} \frac{\partial g(\mathbf{q},\mathbf{r})}{\partial n}\frac{\partial g^*(\mathbf{q}',\mathbf{r})}{\partial n} &= \left(\mathrm{j}k + \frac{1}{r}\right)\left(-\mathrm{j}k^* + \frac{1}{r'}\right)\frac{\mathrm{e}^{-\mathrm{j}(kr-k^*r')}}{16\pi^2 rr'}(\mathbf{u}'\cdot\mathbf{n}_{\mathbf{q}'})(\mathbf{u}\cdot\mathbf{n}_{\mathbf{q}}) \\ &= -\left(\mathrm{j}k + \frac{1}{r}\right)\left(-\mathrm{j}k^* + \frac{1}{r'}\right)\frac{\mathrm{e}^{-\mathrm{j}k_0(r-r')}\mathrm{e}^{-m/2(r+r')}}{16\pi^2 rr'}(\mathbf{u}'\cdot\mathbf{n}_{\mathbf{q}'})(\mathbf{u}\cdot\mathbf{n}_{\mathbf{q}}), \end{aligned} \tag{A.5}$$

$$\begin{aligned} g(\mathbf{q},\mathbf{r})\frac{\partial g^*(\mathbf{q}',\mathbf{r})}{\partial n} &= -\left(-\mathrm{j}k^* + \frac{1}{r'}\right)\frac{\mathrm{e}^{-\mathrm{j}(kr-k^*r')}}{16\pi^2 rr'}(\mathbf{u}'\cdot\mathbf{n}_{\mathbf{q}'}) \\ &= -\left(-\mathrm{j}k^* + \frac{1}{r'}\right)\frac{\mathrm{e}^{-\mathrm{j}k_0(r-r')}\mathrm{e}^{-m/2(r+r')}}{16\pi^2 rr'}(\mathbf{u}'\cdot\mathbf{n}_{\mathbf{q}'}). \end{aligned} \tag{A.6}$$

Using the far-field assumption which states that $kr\gg 1$, $r\simeq r'$ and thus $m/2(r+r')\simeq mr$, the previous equations can be simplified as

$$g(\mathbf{q},\mathbf{r})g^*(\mathbf{q},\mathbf{r}) \simeq \frac{\mathrm{e}^{-\mathrm{j}k_0(r-r')}\mathrm{e}^{-mr}}{16\pi^2 rr'}, \tag{A.7}$$

$$\frac{\partial g(\mathbf{q},\mathbf{r})}{\partial n}\frac{\partial g^*(\mathbf{q}',\mathbf{r})}{\partial n} \simeq k^2 \frac{\mathrm{e}^{-\mathrm{j}k_0(r-r')}\mathrm{e}^{-mr}}{16\pi^2 rr'}(\mathbf{u}'\cdot\mathbf{n}_{\mathbf{q}'})(\mathbf{u}\cdot\mathbf{n}_{\mathbf{q}}), \tag{A.8}$$

$$g(\mathbf{q},\mathbf{r})\frac{\partial g^*(\mathbf{q}',\mathbf{r})}{\partial n} \simeq \mathrm{j}k^* \frac{\mathrm{e}^{-\mathrm{j}k_0(r-r')}\mathrm{e}^{-mr}}{16\pi^2 rr'}(\mathbf{u}'\cdot\mathbf{n}_{\mathbf{q}'}). \tag{A.9}$$

Appendix B

This appendix is concerned with the formulation of the acoustical energy density or intensity for a problem which is solved using geometrical acoustics modelling. Sound waves are assumed to propagate like rays, and the principles of geometrical acoustics specify the linear variation of phase along a ray and the energy conservation inside a ray tube. The field amplitude is predicted using the energy conservation law. Let consider a wavefront defined by the radius of curvature ρ_1 in the xy-plane and ρ_2 in the xz-plane (Fig. 10). On the wavefront at a distance r (resp. $r+\mathrm{d}r$), the radius of curvature are ρ_1+r and ρ_2+r (resp. $\rho_1+r+\mathrm{d}r$ et $\rho_2+r+\mathrm{d}r$). An infinitesimal ray tube crossing the wavefronts define on each of them an infinitesimal curvilinear rectangle and the power between the two rectangles is conserved. The ingoing power crossing the first wavefront at the distance r is written as

$$\mathrm{d}P_{\mathrm{in}} = I(r)\,\mathrm{d}S(r), \tag{B.1}$$

where I is the acoustical intensity and $\mathrm{d}S(r)=(\rho_1+r)(\rho_2+r)\sin\theta\,\mathrm{d}\theta\,\mathrm{d}\phi$ is the surface of the rectangle described on the wavefront. In the same way, the outgoing power crossing the second wavefront at the distance $r+\mathrm{d}r$ can be written as

$$\mathrm{d}P_{\mathrm{out}} = I(r+\mathrm{d}r)\,\mathrm{d}S(r+\mathrm{d}r), \tag{B.2}$$

with $\mathrm{d}S(r+\mathrm{d}r)=(\rho_1+r+\mathrm{d}r)(\rho_2+r+\mathrm{d}r)\sin\theta\,\mathrm{d}\theta\,\mathrm{d}\phi$. A dissipation term proportional to the ingoing intensity through a coefficient m represents the energy loss by unit length. Thus, the outgoing power is expressed as

$$\begin{aligned}\mathrm{d}P_{\mathrm{out}} = {} & I(r+\mathrm{d}r)(\rho_1+r+\mathrm{d}r)(\rho_2+r+\mathrm{d}r)\sin\theta\,\mathrm{d}\theta\,\mathrm{d}\phi \\ & + mI(r)(\rho_1+r)(\rho_2+r)\,\mathrm{d}r\sin\theta\,\mathrm{d}\theta\,\mathrm{d}\phi.\end{aligned} \tag{B.3}$$

The conservation of energy means that $\mathrm{d}P_{\mathrm{in}}=\mathrm{d}P_{\mathrm{out}}$, and the following differential equation taking into account only the first-order terms can be written:

$$\frac{\mathrm{d}I}{\mathrm{d}r}+\left(\frac{1}{\rho_1+r}+\frac{1}{\rho_2+r}\right)I(r)+mI(r)=0, \tag{B.4}$$

with the solution,

$$I(r)=I(0)\frac{\rho_1\rho_2}{(\rho_1+r)(\rho_2+r)}\mathrm{e}^{-mr}. \tag{B.5}$$

$\rho_1=\rho_2$ for spherical waves, $\rho_2\to\infty$ for cylindrical waves and $\rho_1\to\infty$, $\rho_2\to\infty$ for plane waves. Writing Eq. (B.5) as $I(r)=\sigma H(r)$ (Eq. (2)), the amplitude of the fictitious source σ emitting the ray is constant along the ray. Finally, to solve the vibroacoustic problem in a geometrical way, the strength of the equivalent sources

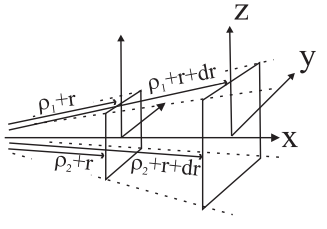

Fig. 10. Energy conservation law inside a ray tube between r and $r+\mathrm{d}r$.

should not depend on the distance from the source point but only on the direction of each ray which is the direction of emission.

References

[1] Sysnoise rev. 5.5 User's Manual, LMS International, Leuven, Belgium, 2000.

[2] L.G. Copley, Integral equation method for radiation from vibrating bodies, *Journal of the Acoustical Society of America* 41 (4) (1967) 807–816.

[3] M. Viktorovitch, F. Thouverez, L. Jezequel, A new random boundary element formulation applied to high frequency phenomena, *Journal of Sound and Vibration* 223 (2) (1999) 273–296.

[4] M. Viktorovitch, F. Thouverez, L. Jezequel, An integral formulation with random parameters adapted to the study of the vibrational behavior of structures in the middle- and high-frequency field, *Journal of Sound and Vibration* 247 (3) (2001) 431–452.

[5] J.-L. Guyader, T. Loyau, Sound radiation from structures: the frequency averaged quadratic pressure approach, *Proceedings of InterNoise*, Vol. 3, Liverpool, UK, July 30–August 2, 1996, pp. 1267–1272.

[6] J.-L. Guyader, T. Loyau, The Frequency Averaged Quadratic Pressure: A method for calculating the noise emitted by structures and for localising the acoustic sources, *Acta Acustica—Acustica* 86 (2000) 1021–1027.

[7] J.-L. Guyader, Integral equation to predict frequency averaged quadratic pressure radiated from structures, *Proceedings of the International Congress on Acoustics*, Kyoto, Japan, April 4–9, 2004 on CD-ROM.

[8] J.-L. Guyader, Integral equation for frequency averaged quadratic pressure, *Acta Acustica—Acustica* 90 (2004) 232–245.

[9] J.-K. Kim, J.-G. Ih, A simplified acoustic boundary element method for the prediction of the acoustic field at high-frequency bands, *Proceedings of the Eighth International Congress on Sound and Vibration*, Hong Kong, China, July 2–6, 2001, pp. 1421–1426.

[10] J.-K. Kim, J.-G. Ih, Prediction of sound level at high-frequency bands by means of a simplified boundary element method, *Journal of the Acoustical Society of America* 112 (6) (2002) 2645–2655.

[11] J.-K. Kim, J.-G. Ih, Prediction of high-frequency sound radiation from muffler jacket using a simplified BEM, *Proceedings of InterNoise*, Seogwipo, Korea, August 25–28, 2003 on CD-ROM.

[12] A. Wang, N. Vlahopoulos, An energy boundary element formulation for sound radiation at high frequency, *Proceedings of InterNoise*, Dearborn, MI, USA, August 19–21, 2002 on CD-ROM.

[13] A. Wang, N. Vlahopoulos, K. Wu, Development of an energy boundary element formulation for computing high-frequency sound radiation from incoherent intensity boundary conditions, *Journal of Sound and Vibration* 278 (1–2) 413–436.

[14] G.H. Koopmann, L. Song, J. Fahnline, A method for computing acoustic fields based on the principle of wave superposition, *Journal of the Acoustical Society of America* 86 (6) (1989) 2433–2438.

[15] T. Tomilina, The equivalent sources approach to acoustical design of forced vibrating structures, *Proceedings of InterNoise*, Leuven, Belgium, August 24–26, 1993, pp. 1597–1600.

[16] M. Ochmann, The source simulation technique for acoustic radiation problems, *Acustica* 81 (1995) 512–527.

[17] D.W. Herrin, T.W. Wu, A.F. Seybert, The energy source simulation method, *Journal of Sound and Vibration* 278 (1–2) (2004) 135–153.

[18] R.S. Langley, P. Bremner, A hybrid method for the vibration analysis of complex structural–acoustic systems, *Journal of the Acoustical Society of America* 105 (3) (1999) 1657–1671.

[19] H.W. Lee, S.H. Hong, Y.H. Park, Radiation noise analysis using the results of power flow finite element method, *Proceedings of InterNoise*, The Hague, The Netherlands, August 27–30, 2001 on CD-ROM.

[20] V. Jayachandran, M. Bonhila, A hybrid SEA/modal technique for modeling structural–acoustic interior noise in rotorcraft, *Journal of the Acoustical Society of America* 113 (3) (2003) 1448–1454.

[21] V. Cotoni, A. Le Bot, Radiation of plane structures at high frequency using an energy method, *International Journal of Acoustics and Vibration* 6 (2001) 209–214.

[22] A. Le Bot, A. Bocquillet, Comparison of an integral equation on energy and the ray-tracing technique for room acoustics, *Journal of the Acoustical Society of America* 108 (2000) 1732–1740.

[23] L.P. Franzoni, D.B. Bliss, J.W. Rouse, An acoustic boundary element method based on energy and intensity variables for prediction of high-frequency broadband sound fields, *Journal of the Acoustical Society of America* 110 (6) (2001) 3071–3080.

[24] A. Le Bot, Comparison of vibrational conductivity and radiative energy transfer methods, *Journal of Sound and Vibration* 283 (2005) 135–151.

[25] C. Lesueur, Rayonnement acoustique des structures—Vibroacoustique, Interactions fluide-structure, n°66 Collection de la Direction des Etudes et Recherches d'Electricité de France, Eyrolles, Paris, 1988.

[26] A. Le Bot, A functional equation for the specular reflection of rays, *Journal of the Acoustical Society of America* 112 (4) (2002) 1276–1287.

[27] E. Reboul, A. Le Bot, J. Perret-Liaudet, Radiative transfer equation for multiple diffraction, *Journal of the Acoustical Society of America* 118 (3) (2005) 1326–1334.

[28] M. Norton, *Fundamentals of Noise and Vibration Analysis for Engineers*, Cambridge University Press, Cambridge, 1989.